Neuroscience Informatics 3 (2023) 100118

Contents lists available at ScienceDirect

Neuroscience Informatics

journal homepage: www.elsevier.com/locate/neuri

Original article

# A connectome-based deep learning approach for Early MCI and MCI detection using structural brain networks

Shayan Kolahkaj, Hoda Zare *

*Medical Physics Research Center, Mashhad University of Medical Sciences, Mashhad, Iran*

ARTICLE INFO

*Article history:*
Received 2 June 2022
Received in revised form 30 December 2022
Accepted 20 January 2023

*Keywords:*
Mild cognitive impairment
Diffusion tensor imaging
Connectomes
Deep learning
Convolutional neural networks

ABSTRACT

Precise detection of Alzheimer's disease (AD), especially at the early stages, i.e., early mild cognitive impairment (EMCI) and MCI, allows the physicians to promptly intervene to prevent the progression to advanced stages. However, identification of such stages using non-invasive brain imaging techniques like DWI, remains one of the most challenging tasks due to the subtle and mild changes in the brain structures of the subjects. Findings from previous studies suggested that topological organization alterations occur in the DTI-derived structural connectomes in MCI patients. Therefore, for improving diagnosis performance, we presented a connectome-based deep learning architecture based on BrainNet Convolutional neural network (CNN) model. The proposed model automatically extracts hidden topological features from structural networks using specially-designed convolutional filters. Experiments on 360 subjects, including 120 subjects with EMCI, 120 subjects with MCI and, 120 normal controls (NCs), with both T1-weighted MRI and DWI scans from the Alzheimer's Disease Neuroimaging Initiative (ADNI), provided the highest binary classification accuracies of 0.96, 0.98, and 0.95 for NC/EMCI, NC/MCI and EMCI/MCI respectively.

In addition, we also investigated the effect of different atlas sizes and fiber descriptors as edge weights on the discriminative ability of the classification performance. Experimental results indicate that our approach exhibited superior performance to previous methods and performed effectively without any prior complex feature engineering and regardless the variability of imaging acquisition protocols and medical scanners.

Finally, we observed that DTI-based graph representation of brain regions connections preserve important but hidden connectivity pattern information to discriminate between clinical profiles, and our proposed approach could be easily extended to other neurodegenerative and neuropsychiatric diseases.



## 1. Introduction

Alzheimer's disease (AD) is an irreversible, degenerative neurological disorder that causes progressive deterioration of the brain connectivity network followed by a decline in cognitive abilities. It is the most prevalent cause of dementia, accounting for about 60% to 70% of all dementia cases in the World [1–3]. Although there is no way to stop the disease when it is too advanced, studies show that its progression can be slowed down or interrupted if identified at an early stage [4]. Mild cognitive impairment (MCI) is the first sign of dementia which holds a great potential to convert into Alzheimer's disease within the subsequent 3–5 years [5,6]. On the trajectory leading to Alzheimer's Disease, Early mild cognitive impairment (EMCI), another prodromal stage of AD, is considered as the earliest and relatively asymptomatic diagnostic group, and also a transitional stage to AD [7]. Investigating EMCI subjects is also particularly important alongside the MCI subjects. This is primarily because 27% of those with EMCI have been recorded to convert to AD [8]. Subsequently, identification of both Early MCI and MCI is a pivotal step to early-stage detection of dementia, making it possible for clinicians to provide early intervention and develop future treatments. However, an accurate and robust diagnostic classification is considered highly challenging due to the minimum variance between the early stages of Alzheimer's Disease especially, EMCI and MCI patients.

Some advanced neuroimaging techniques, such as diffusion tensor imaging (DTI) can detect the age-related alterations in the topology of the brain structural network. This is thought to result from white matter microstructure degeneration in AD and MCI due to demyelination, gliosis, severe fiber loss and etc. [9,10,42,43] Graph theory is a robust body of mathematical knowledge that

* Corresponding author.
*E-mail address:* Zareh@mums.ac.ir (H. Zare).

https://doi.org/10.1016/j.neuri.2023.100118

enables representing the brain as a large-scale complex network of interacting elements, the so-called "human connectome" [11]. These macroscopic-level connectomes can be constructed from diffusion MRI tractography of white matter through assigning different anatomical regions as nodes and the white matter fiber connections between the regions as edges. Once the brain network is generated, many graph-based measures such as small-worldness, modular structure, network efficiency and centrality can be used to elucidate the underlying topological organization of the network. There is growing evidence showing that these graph metrics demonstrated decrease in topological efficiency in AD and MCI patients, which is associated with synaptic damage and cognitive decline [12,13]. However, in healthy subjects, the topological organization of the connectomes is highly efficient in combination with a high level of segregation and integration [14]. These findings indicate the tremendous potential of connectome-based biomarkers in early detection of AD, for the early identification of dementia and diagnostic groups like early MCI and MCI.

Over the past decade, a large number of studies attempted to develop machine learning and deep learning methods to look at the potential of diffusion-weighted imaging for AD stage classification. Most of these studies have used statistical and traditional machine learning methods along with handcrafted features which are extracted from neuroimaging data and make the experiments difficult to reproduce. Prasad et al. [15] used connectivity matrices of 68 $\times$ 68 and extracted network metrics from 68 brain regions. Graph or network metrics are then used as input of support vector machine (SVM) to classify early MCI and NC, achieving an accuracy of 59%.

These traditional machine learning methods are likely to fail in challenging scenarios such as identifying EMCI, because of their inability to capture high-level features in DW images.

Another approach that has recently received much attention in the neuroimaging domain and brain data analysis is deep learning algorithms. In deep learning-based techniques, automatic feature extraction enables models to extract meaningful and complex hidden features within the input dataset. Parameter sharing in neural networks is another advantage of these techniques in which the number of unknown parameters reduces significantly, leading to improving computational efficiency. (Khvostikov et al. [16]) Extracted ROI-based hippocampus volumes in structural MRI and DTI modality and then used a 3D deep neural network to distinguish Alzheimer's disease and Mild cognitive impairment. An accuracy of 0.68 had been obtained for the ternary AD/MCI/NC classification problem.

However, deeper neural network architectures require more data, and consequently a substantial time for training. The main issue, however, is that, in general, data in the neuroimaging domain (especially DWI), is not adequately available. Due to this reason, several research studies have utilized transfer learning techniques based on popular deep learning networks to address the lack of data. "Transfer Learning" or fine-tuning is a phenomenon which is reusing the weights of a previously trained model that is initially implemented for other application domains [17]. This approach can be implemented by freezing network layers (mostly intermediate layers). Kang et al. [18] proposed a convolutional neural network based on transfer learning technique to extract features of multi-modality images (sMRI and DTI) and utilized an SVM classifier for binary classification of EMCI and Normal Control subjects. They reported an average accuracy and specificity of 94% and of 92% respectively for a dataset of 70 EMCI and 50 NC subjects. Marzban et al. [19] employed a 2D CNN model and extracted diffusion maps (FA and MD) and gray matter volumes as input images for detecting MCI and AD and achieved an accuracy of 79.6% and 93.5% respectively.

A handful of studies tried to apply DTI tractography in combination with graph theory to identify AD stages through deep learning algorithms. For example, Lella et al. [20] developed an ensemble model based on three topological properties of the network (weights; shortest path length and communicability), measured from DTI data to identify MCI. Sheng et al. [21] in another study, used handcrafted network measures such as strength (S), degree, local efficiency (LE) and subgraph centrality (SC) from fMRI data to a binary classification of four AD stages. SVM is then used for feature selection before feeding the final features to a five-layer Deep Neural Network model.

Conversely, the connectome data that is derived from applying graph theory to DTI streamlines cannot directly be used as input to Neural network filters due to the inherently topological information that exists between graph or network elements. This is the point where graph neural networks (GNNs) [22] come in. Graph Convolutional Neural Networks (GCNN) [23] are special cases of GNNs that generalize the operation of convolution from grid-like data (i.e. images) to graph structured data via graph Fourier transform [24]. Such networks can automatically extract and use non-linear features of graphs for the classification task, which is significantly superior to low-level linear methods. Song et al. [25] presented a multi-class Graph CNN architecture for direct usage of structural connectivity matrices as input, reported an average accuracy of 89% in four stage classification for a dataset consisting of 12 subjects for each class.

On the other hand, however, GCNs, while increasingly popular, also seem under performed to use with connectome data, since the relationships between the nearest pixels on a channel can only to be captured, and therefore the most valuable information exists between distant nodes in an adjacency matrix might get lost. In this context, deep neural networks that can exploit the topological characteristics of brain networks have been recently explored. In 2017, BrainNetCNN was proposed to exploit hidden topological network features for predicting the neurodevelopment outcome scores in preterm infants [26]. This type of neural network mainly, is a novel type of CNN and can preserve topological information in connectomic data while training connectivity matrices using three specially-developed filters. The filtering layers are listed as follows: 1) edge-to-edge (E2E) layer, 2) edge-to-node (E2N) layer and 3) node-to-graph (N2G) layer.

In addition, two recent studies also demonstrated that spectral GCN and traditional CNN is considerably less-optimal than the BrainnetCNN, one in resting-state functional connectivity for behavioral prediction [27] and another one in sex prediction on structural connectomes [28].

In this work, we further propose a modified version of the BrainNetCNN to address multi-class and binary classification tasks of three AD prodromal stages, including early MCI, MCI and Health controls. To our best knowledge, we are the first to employ BrainnetCNN for early MCI and MCI classification using structural brain connectomes calculated from CSD-based probabilistic tractography. Finally, we elaborated structural network representations by applying a range of fiber descriptors such as the normalized number of fibers, fiber integrity (or "fractional anisotropy"), fiber length and fiber density between pairs of anatomical brain regions to find the best weighted representations of structural connectome in terms of robustness and precision in the classification process.

## 2. Material and methods

### 2.1. Data acquisition

Structural MRI and DTI data for normal controls (NC), EMCI and MCI subjects used in this study are obtained from the Alzheimer's Disease Neuroimaging Initiative (ADNI) database [41]. It launched

**Table 1**
The clinical and demographic characteristics of participants with NC, EMCI, and MCI groups.

| | NC | EMCI | MCI |
|---|---|---|---|
| Number | 120 | 120 | 120 |
| Gender (F/M) | 50/70 | 42/78 | 47/73 |
| Age (year) | 75.26 ± 6.52 | 72.9±8.3 | 73.47 ± 7.23 |
| MMSE | 29.18 ± 0.98 | 27.86±1.66 | 26.88 ± 1.76 |
| GE/SIEMENS/PHILIPS | 46/64/10 | 68/41/11 | 14/87/19 |

in 2003 as a public-private partnership, led by Principal Investigator Michael W. Weiner, MD. ADNI is a multisite, longitudinal study and its main goal is to detect biomarkers for clinical use and to test whether serial MRI, PET, other biological markers, clinical and neuropsychological assessment can be combined to measure the progression of MCI and early stages of AD.

In particular, we analyzed a balanced cohort of 360 subjects grouped into 120 NC, 120 EMCI and 120 MCI. The dataset is labeled as one of the AD prodromal stages according to their ADNI classification. The criteria for the classification of the subjects was based on mini-mental state examination (MMSE) and global clinical dementia rating (CDR) scores [29]. For the EMCI cohort, the subject must have a subjective memory concern as reported by the subject, study partner, or clinician. Both early MCI and MCI have an MMSE score between 24 and 30; a Clinical Dementia Rating (CDR) score of 0.5, to which the participants reported memory complaints with no significant functional impairment. Therefore, to distinguish between the EMCI and MCI, objective memory deficits on the Wechsler Memory-Scale-Logical Memory II test was used with scores between 0.5SD–1.5SD indicating early MCI and lower than 1.5SD below the norm indicative of MCI, which ensured no overlap between the clinical profiles. Table 1 shows the detailed demographic information of the subjects used in this study. We included the subjects whose DWI and T1-weighted MRI scans were available at baseline. A variety of different 3T Medical Systems manufactured by GE, Siemens and Philips were used for whole-brain MRI scanning for all the participants. 46 separate images were acquired for each DTI scan: 5 T1-weighted images with no diffusion sensitization (b0 images) and 41 diffusion-weighted images (b = 1000 s/mm2). For DWI scans, two different acquisition protocols are described: 1) Axial DTI and 2) Enhanced Axial DTI according to the "IDA_MR_Metadata_Listing.csv" file on the ADNI website. More details about the ADNI MRI scanners data acquisition protocols can be seen on ADNI's official webpage [41].

### 2.2. Preprocessing

Basically, for computing the structural connectivity matrix, the image processing steps were divided into two pathways that converge at the registration step for a final pathway.

Firstly, the cerebral cortex for each subject was parcellated from high resolution anatomical T1-weighted volume into 129, 234 and 463 brain regions using Freesurfer software and the Lausanne 2008 (hierarchical multi-resolution parcellation scheme) [30]. The atlas was originally created to produce multiple acceptable resolution and approximately equal brain regions (about 1.5 $cm^2$) based on Desikan-Killiany and Hagmann atlases. This anatomical reference information of each region would further be used to define network nodes. More precisely, intensity normalization, motion correction, non-brain tissue removal, skull stripping and brain mask generation are also done by Freesurfer's recon-all function.

Diffusion MRI scans on the other hand were first corrected for susceptibility distortions and eddy current induced by gradients and head motion [33] using the FSL software package [31].

Then, the parcellated images created during the segmentation step have co-registered to the non-diffusion-weighted (b0) average of dMRI volumes using affine transformation with FLIRT. Finally, after structural network nodes were determined using 129, 234, and 463 parcellation scales, voxel-wise fiber orientation distributions (FOD) were computed using constrained spherical deconvolution (CSD) and will serve later on to perform tractography. The MRtrix package was employed to reconstruct whole-brain fiber streamlines using probabilistic tractography by (iFOD2) function in MRtix software [32], which improves reconstruction accuracy but has not been broadly used in connectome analyses and AD staging.

A set of one million streamlines in the brain were generated using 5tt maps and randomly seeding the brain mask within the GM/WM interface with the following parameters: default step size of (0.5), curvature angle: 45° and FOD amplitude threshold: 0.2. The so-called 5-tissue type segmented images (5TT) were also provided to the anatomically-constrained tractography (ACT) which allows us to detect the GM/WM interface directly. In 5TT format, the brain tissue is categorized into 5 different tissue types: CSF, WM, cortical gray matter, subcortical gray matter and pathological tissue. The ACT method overall improves tractography reconstruction results using anatomical information through imposing a limitation for the streamline generation [34]. Each of the whole-brain structural connectomes took around 18 hours to calculate and a SIFT tract filtering method had been used to remove false positive tracts for each tractogram. The SIFT method tries to improve the agreement between the generated streamlines and the diffusion data to decrease computational artifacts by eliminating fibers that are too long and too short. It was recently shown that the SIFT method leads to a more reliable and biologically meaningful connectome [35].

### 2.3. Structural connectivity (SC) matrix construction

For constructing white matter structural matrices which are symmetric by nature, fiber counting was performed on each parcellated brain template and WM tracts of the probabilistic tractography. The Lausanne 2008 atlas segmented the brain into 129, 234 and 463 regions, and so the consequent generated structural connectivity networks are weighted matrices with dimension of $129 \times 129$ and $234 \times 234$ and $463 \times 463$ respectively. The value of each element within the matrix represents one of the three fiber descriptors (normalized number of fibers, FA mean, fiber length and fiber density) with two endpoints located in two distinct regions. Eventually, the connectivity matrices were created for each subject using a variety of fiber descriptors such as fiber integrity as measured by mean fractional anisotropy (FA mean), fiber length, fiber density and the normalized number of fibers (calculated as the ratio of the number of fibers and the voxel number). These quantitative descriptors serve as edge weights, connecting parcellated regions in the brain network. The schematic methodology of data processing steps is summarized in Fig. 1.

### 2.4. Connectome augmentation

A dataset of 360 adjacency matrices for training a deep neural network model is considered relatively low even in the presence of powerful convolutional filters. This is due to the high number of parameters that need to be learned in a deep neural network. Therefore, we employed an oversampling SMOTE technique

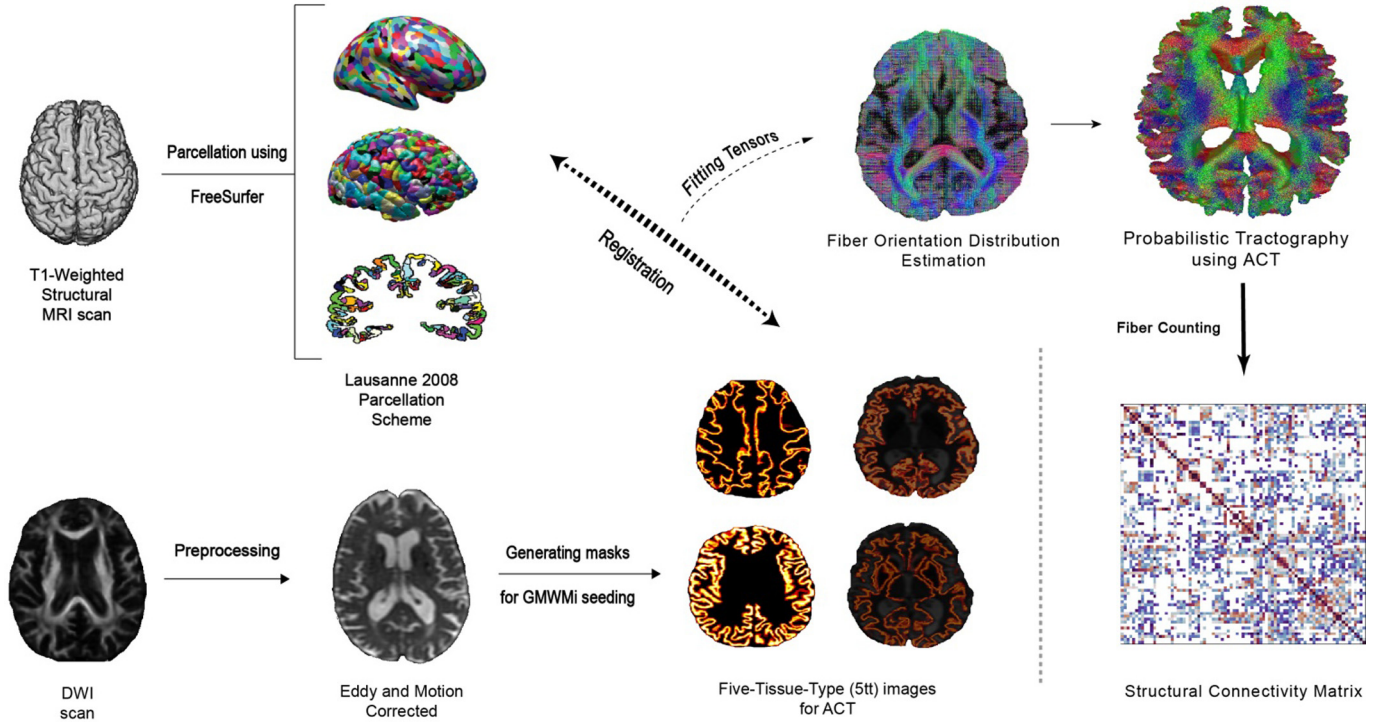


**Fig. 1.** Image processing pipeline. DWI and T1-weighted scans underwent several processing steps to generate a structural connectivity matrix as the final output.

to augment the number of connectomes in each class. We utilized SMOTE to generate five more samples for each connectome synthetically and, as a result, enhance the prediction efficiency of the model. The constructed adjacency matrices used to build the following human connectome dataset for training a BrainnetCNN model. Finally, our dataset was split into a train set and test set with a ratio of 7:3.

### *2.5. Proposed deep learning architecture*

Deep neural networks and particularly convolutional neural networks (CNNs) have had great success in many different domains, and this is due to the increased availability of GPU computing and large-scale public datasets, and in part to the potential of learning representations from grid-like data structures (i.e. images) through convolutional filters. However, the conventional formulation of traditional CNNs is purely limited to grid-like data structures like images; thus they are not capable of capturing sophisticated topological neighborhood features, and since the human connectome is inherently represented as a graph rather than a grid, CNNs are inefficient when dealing with data which are presented in an irregular grid or more generally, in a non-Euclidean space. This is due to the inherent characteristic of adjacency matrix where local neighbors of a brain region (or a node in the adjacency matrix) are placed along horizontal rows and vertical columns. Hence, many machine learning or deep learning techniques are limited in their capability to capture relationships between clinical/behavioral variables and connectomic features because of their dependence on shallow or linear algorithms.

BrainnetCNN was specifically developed by Kawahara et al. in 2017 to predict preterm infant Age and Neurodevelopmental Outcome scores [26]. The main idea was to extend convolutional neural networks (CNNs) to leverage the topological structure of brain networks and make it possible to utilize graph-structured (i.e. connectome) data directly. Furthermore, BrainnetCNN is making it possible to exploit the topological local characteristics of brain networks (Fig. 2). It consists of specially-designed edge-to-edge (E2E), edge-to-node (E2N) and node-to-graph (N2G) convolutional layer types for brain network data. Each layer in fact, is a unique filter that is a particular case of more general convolutional filters that can have meaningful interpretations in terms of network topology.

**E2E layer:** In contrast to the box shape filters in CNNs, BrainnetCNN utilizes some cross shape filters in the E2E layer with the dimension of 1 x d and d x 1 (for an input connectome with the size of d x d) to combine signals from direct neighbors. The edge-to-edge layer (E2E), which is the first layer of the BrainnetCNN is analogous to a traditional convolutional layer and can only be applied before edge-to-node (E2N) layer. In fact, in both E2E layer and convolutional layers, the data is being filtered locally in small patches. Defining the convolutional layer in terms of spatial locality and the E2E layer in terms of topological locality indicates the difference between these two types of filtering layers. Moreover, at the E2E layer, the weighted sum of edges in the network that shares a node is calculated by the above-mentioned cross-shaped filter and produces M feature maps. Since a connectome network has no boundaries in terms of topological properties, the output feature maps of the E2E layer are the same size as input connectome networks. These feature maps, thus, are the input of the E2N layer (Fig. 3).

**E2N layer:** Applying the cross-shaped filter to only the diagonal elements of the input feature map is the key distinguishing attribute of the E2N layer. It takes in a d x d feature map and outputs a unique vector with the size of d x 1. Thus, in other words, the layer is designed for reducing the input dimensionality of extracted features.

**N2G layer:** This is a fully-connected layer connected to the previous layer (E2N layer). Fully connected (FC) layers in this case reduce the number of features down to two output score predictions.

For each output feature map, M, the Node-to-Edge filter performs a 1D spatial convolution and reduces the spatial dimensions of the original input.

In Kawahara's study, a regression task for prediction, performed over a single class and it cannot be directly used in binary or

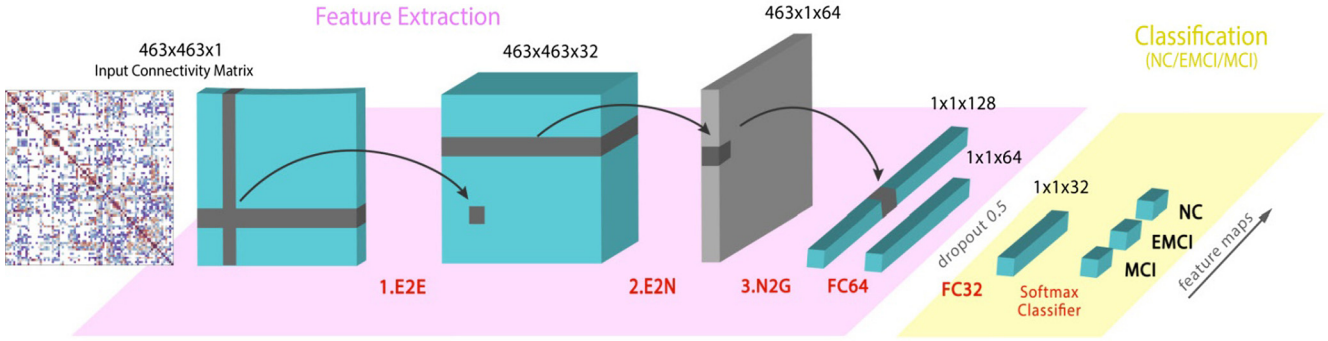


**Fig. 2.** Schematic representation of the proposed model architecture. Modified BrainnetCNN consists of three blocks, each representing the input and/or output of the numbered filter layers. The input connectivity matrix is first convolved with a multiple numbers of E2E filters which weight edges of the brain network. The output then is convolved with some E2N filters which assign each brain region a weighted sum of its edges. The N2G in this architecture assigns a single response based on all the weighted nodes and eventually, the Fully-connected layer (FC) reduces the number of features down to three class class-membership probability.

multi-class classification. In this current work, we have extended BrainnetCNN method to determine the discriminative capability of using CSD-probabilistic structural connectivity matrix in separating EMCI and MCI patients from normal controls (NCs). This is achieved through converting the original regression task in Kawahara's method to a classification task, in which, the proposed neural network classifies the structural network matrices into one of the three disease class labels. In order to reduce the number of trainable parameters and the dimensionality of the input, we used 8 E2E layers and 16 E2N layers, each followed by a leaky rectified linear unit (denoted LeakyReLU). The output layer is a single fully-connected node-to-graph (N2G) layer and carries out the classification operation. As aforementioned above, the N2G fully-connected layer is our classifier whose output dimensionality is equal to the number of possible answers.

The probability for each class-membership is computed by applying a softmax function for the multi-class tasks and a sigmoid function for the binary tasks to the output vector of the final layer.

### 2.6. Experimental setting

Modified BrainnetCNN network implemented using Keras deep learning suite and TensorflowBackend, via the Adam optimizer [36] with a learning rate of $10^{-4}$ and a batch size of 4. All the experiments are conducted on a machine with Ubuntu 20.04, an NVIDIA GeForce RTX 2060 GPU with dedicated 6 GB memory along side an Intel i7 Central Processing Unit (CPU) 64 bits. To reduce the overfitting, we employed an early stopping strategy and added some dropout layers after each main layer in the architecture. Dropout layers work by setting the output of each hidden neuron in the neural network to zero with a specific probability [37]. The whole process thus, is discarding some neurons so they will not activate during forward pass and backpropagation, thereby enhancing generalization performance.

## 3. Results

In this section, we show some experimental results on training and evaluation for a ternary NC/EMCI/MCI and three binary (EMCI/NC, MCI/NC, EMCI/MCI EMCI/MCI) classification tasks to identify corresponding classes.

The obtained results are reported in Table 2. Furthermore, to investigate the impact of choices of different fiber descriptors strategies on classification tasks, we also evaluated our proposed model based on different fiber descriptors such as fiber density, average fractional anisotropy (FA mean), fiber length and the normalized number of fibers.

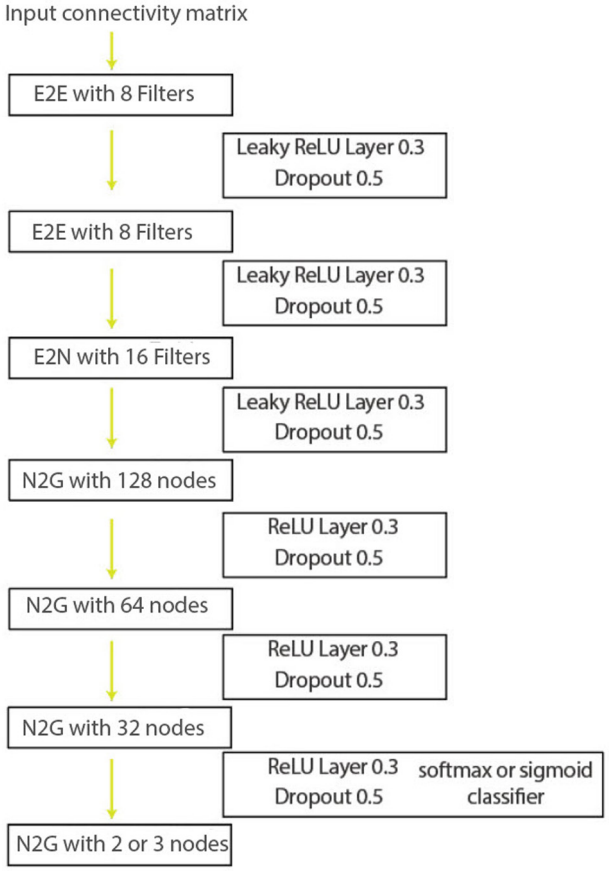


**Fig. 3.** Architecture of modified BrainnetCNN neural network model.

Eventually, four standard metrics (accuracy, precision, recall and F1-measure) were considered to assess the performance of classification results. These metrics are defined as:

$$Accuracy = \frac{TP + TN}{TP + TN + FP + FN}$$

$$Precision = Confidence = \frac{TP}{TP + FP}$$

$$Sensitivity = Recall = \frac{TP}{TP + FN}$$

$$F1 - Score = \frac{2 * Precision * Recall}{Precision + Recall}$$

Where TP, TN, FP, and FN are denoted as the true positive, true negative, false positive, and false negative, respectively and are

**Table 2**
Classification performance results of the proposed method for distinguishing EMCI and MCI from NC.

| Task | Atlas size | Accuracy | Precision | Recall | F1-score |
|---|---|---|---|---|---|
| FA mean | | | | | |
| NC vs EMCI | **N=129** | 0.92 | 0.91 | 0.93 | 0.92 |
| | **N=234** | 0.90 | 0.89 | 0.92 | 0.90 |
| | **N=463** | **0.96** | **0.94** | **0.96** | **0.95** |
| NC vs MCI | **N=129** | 0.89 | 0.90 | 0.88 | 0.89 |
| | **N=234** | 0.93 | 0.92 | 0.93 | 0.92 |
| | **N=463** | **0.98** | **0.98** | **0.98** | **0.98** |
| EMCI vs MCI | **N=129** | 0.86 | 0.84 | 0.84 | 0.84 |
| | **N=234** | 0.88 | 0.88 | 0.88 | 0.88 |
| | **N=463** | **0.96** | **0.95** | **0.93** | **0.94** |
| NC/EMCI/MCI | **N=129** | 0.85 | 0.86 | 0.84 | 0.85 |
| | **N=234** | 0.86 | 0.89 | 0.84 | 0.86 |
| | **N=463** | **0.92** | **0.92** | **0.92** | **0.92** |
| Normalized Number of Fibers | | | | | |
| NC vs EMCI | **N=129** | 0.88 | 0.87 | 0.89 | 0.88 |
| | **N=234** | 0.90 | 0.88 | 0.92 | 0.90 |
| | **N=463** | **0.92** | **0.92** | **0.93** | **0.92** |
| NC vs MCI | **N=129** | 0.87 | 0.86 | 0.86 | 0.86 |
| | **N=234** | 0.86 | 0.84 | 0.87 | 0.85 |
| | **N=463** | **0.95** | **0.94** | **0.95** | **0.94** |
| EMCI vs MCI | **N=129** | 0.84 | 0.81 | 0.83 | 0.82 |
| | **N=234** | 0.84 | 0.79 | 0.84 | 0.81 |
| | **N=463** | **0.91** | **0.90** | **0.90** | **0.90** |
| NC/EMCI/ MCI | **N=129** | 0.82 | 0.82 | 0.82 | 0.82 |
| | **N=234** | 0.86 | 0.86 | 0.86 | 0.86 |
| | **N=463** | **0.88** | **0.85** | **0.86** | **0.85** |
| Fiber Density | | | | | |
| NC vs EMCI | **N=129** | 0.84 | 0.84 | 0.86 | 0.85 |
| | **N=234** | 0.86 | 0.90 | 0.88 | 0.87 |
| | **N=463** | **0.90** | **0.89** | **0.91** | **0.90** |
| NC vs MCI | **N=129** | 0.87 | 0.84 | 0.86 | 0.85 |
| | **N=234** | 0.84 | 0.83 | 0.84 | 0.83 |
| | **N=463** | **0.94** | **0.92** | **0.93** | **0.93** |
| EMCI vs MCI | **N=129** | 0.87 | 0.86 | 0.85 | 0.85 |
| | **N=234** | 0.90 | 0.90 | 0.89 | 0.89 |
| | **N=463** | **0.95** | **0.94** | **0.92** | **0.93** |
| NC/EMCI/MCI | **N=129** | 0.85 | 0.86 | 0.85 | 0.85 |
| | **N=234** | 0.86 | 0.83 | 0.86 | 0.84 |
| | **N=463** | **0.86** | **0.86** | **0.86** | **0.86** |
| Fiber Length | | | | | |
| NC vs EMCI | **N=129** | 0.85 | 0.85 | 0.85 | 0.85 |
| | **N=234** | 0.84 | 0.85 | 0.84 | 0.84 |
| | **N=463** | **0.87** | **0.86** | **0.87** | **0.86** |
| NC vs MCI | **N=129** | 0.85 | 0.85 | 0.85 | 0.85 |
| | **N=234** | 0.86 | 0.87 | 0.88 | 0.87 |
| | **N=463** | **0.86** | **0.83** | **0.84** | **0.83** |
| EMCI vs MCI | **N=129** | 0.73 | 0.73 | 0.73 | 0.73 |
| | **N=234** | 0.75 | 0.76 | 0.76 | 0.75 |
| | **N=463** | **0.83** | **0.85** | **0.84** | **0.84** |
| NC/EMCI/MCI | **N=129** | 0.77 | 0.75 | 0.74 | 0.74 |
| | **N=234** | 0.79 | 0.79 | 0.79 | 0.79 |
| | **N=463** | **0.83** | **0.83** | **0.83** | **0.83** |

derived from the confusion matrix. TP in our case, indicates the number of Early MCI and MCI patients and TN is the number of Health Controls that are identified correctly. FP on the other hand, refers to the number of subjects falsely identified as EMCI or MCI patients, and FN is the number of health Control subjects that are misclassified.

The best performance of ternary classification's (NC/EMCI/MCI) accuracy, precision, recall, and F1-measure for BrainnetCNN model and weighted connections of average fractional anisotropy between the brain regions was 92%, thereby significantly exceeding the current state-of-the-art methods.

The highest accuracy was obtained in the MCI/NC classification tests using average Fractional Anisotropy edge weights and connectomes made by atlas size of 463. Modified BrainnetCNN were also able to discriminate between EMCI and MCI patients with an optimal performance (accuracy, recall and precision scores higher than 90%; Table 2). In distinguishing EMCI from Normal Control subjects, the proposed approach reached an accuracy, up to about

96%, for FA mean and 92% for normalized number of fibers as edge weight connection, making it by far the highest classification performance achieved so far. Overall, average fiber length descriptor had performed poorly to distinguish between AD stages and was not a reliable descriptor to discriminate between mild stages.

In summary, based on the literature, our classification results indicate that the proposed approach is significantly better than other comparative approaches in both binary and multi-class categorization experiments of EMCI, MCI and NC groups.

## 4. Discussion and conclusion

The present study aimed to evaluate the capability of the novel deep learning technique, BrainnetCNN and DTI-derived brain networks for identifying EMCI and MCI stages efficiently. Overall, most of the previous studies of early MCI diagnosis suffer from several problems such as low robustness and accuracy and heavy handcrafted feature engineering. Therefore, to overcome these issues, we used structural brain connectomes as direct inputs to our modified BrainnetCNN model. We also assessed the influence of four different fiber descriptors on the performance of the proposed model; using average Fractional Anisotropy (FA mean), Fiber density, Fiber length and normalized number of fibers as edge connection between brain parcels in our study, demonstrated that classification results can be significantly affected by the chosen intra-voxel markers. To generate fiber pathways, previous studies have commonly relied upon just a single type of fiber descriptor scheme.

In almost all the classification groups, the performance of the proposed method exceeded that of the baseline approaches, although the differences were larger for higher resolution parcellations.

We found that the 463-node atlas provided higher classification rates than the smaller atlases, suggesting that higher resolution parcellations allow better detection of hidden topological features.

Results suggest that the parcelletation scale with 463 brain regions has achieved the best performance in our model with an accuracy of 98%, making it the most robust sensitive approach. We have demonstrated that the proposed method can predict AD stages with an accuracy that, for EMCI and MCI, matches or improves on the corresponding stages classified with the conventional deep learning methods. While no direct comparison could be made to other neural network-based methods for AD stages prediction, as we found no such method that could be implemented on a BrainnetCNN model directly, the accuracies for EMCI and MCI are comparable with accuracies reported in the literature [18–21].

Another contribution of our work is to highlight the advantage of using the CSD-based (Constrained Spherical Deconvolution) probabilistic tractography to circumvent the limitation of accurately estimating the actual trajectories of white matter in kissing or fanning fibers areas [38,43]. The probabilistic method also shows higher structural reproducibility than the deterministic method in terms of adjacency matrix computation [39].

Our results help to clarify that structural connectome information based on probabilistic tractography fiber descriptors is a valuable and sensitive approach to diagnose dementia and Alzheimer's disease at early stages.

In addition to high sensitivity and accuracy, the proposed approach has several advantages: Firstly, the modified BrainnetCNN has the potential to detect structural deficits and changes associated with early dementia stages and AD. Secondly, in contrast to previous multi-modality fusion methods [16,18,40], we did not utilize multiple neural network models to extract features of the neuroimaging data and then fuse them in the final step. Contrarily, the proposed model, automatically extracts the semantic topological features from the input DTI-derived structural networks and then we fused structural MRI brain regions in our DWI data which are crucial supplements to anatomically-constrained probabilistic tractography (ACT).

As far as we know, this is the first work investigating the direct usage of ACT-based and CSD-based structural connectivity matrices in diagnosis of EMCI and MCI patients. Several previous studies are noted that multi-modality MRI especially DTI and fMRI modalities are much more effective than structural MRI alone for EMCI identification; However, none of them employed techniques such as ACT and CSD probabilistic tractography and fed the derived connectome directly to the neural network model [16,18–20,43].

Interestingly, the predicted classification of EMCI group and classification of Health Controls were highly accurate (96%) in this study, while there were still significant difficulties in classifying both groups within previous studies. This may be due the characteristic features of EMCI with NC are hard to be detected from conventional image analysis and complex feature engineering from multiple neural network models, and capturing the disrupted topological organization of DTI fiber-made brain networks using connectome-based deep neural network models is likely to be the key to distinction between early phases of dementia. The structural brain network, indeed, seems to embody highly discriminative properties characterizing the clinical profiles. However, in reality, there were still some limitations in our study. First, we used a modest dataset size for training and evaluation of our neural network approach which is a common limitation in medical imaging analysis using deep neural networks where there is scarce DTI data available especially for EMCI patients. Second, although the topological features that had the most decisive influence in distinction between patient groups are not able to be discovered due to non-interpretability of the neural network models. However, our proposed model showed superior generalizability across EMCI, MCI and NC subjects and even multiple data acquisition sites. It is also worth to note that the differences in DTI MRI data processing methods used, as well as the differences in experimental setting (e.g., our model trains on substantially less trainable parameters than other approaches) make direct comparisons unclear, and that our major advantage is equipping a deep-learning framework with the proposed element-wise filters.

In summary, the outstanding classification performance achieved in this article again proves that DTI-derived connectomes can act as non-invasive diagnostic biomarkers for early MCI and MCI detection. The robustness of our modified BrainnetCNN model is suitable for further development for clinical usage and future works could address multiple neuroimaging modalities to provide complementary information to d-MRI connectomes.

## Human and animal rights

The authors declare that the work described has been carried out in accordance with the Declaration of Helsinki of the World Medical Association revised in 2013 for experiments involving humans as well as in accordance with the EU Directive 2010/63/EU for animal experiments.

## Funding

This work did not receive any grant from funding agencies in the public, commercial, or not-for-profit sectors.

## Author contributions

All authors attest that they meet the current International Committee of Medical Journal Editors (ICMJE) criteria for Authorship.

## Declaration of competing interest

The authors declare that they have no known competing financial or personal relationships that could be viewed as influencing the work reported in this paper.

## References


[1] J.M. Peters, T. Hummel, T. Kratzsch, J. Lötsch, C. Skarke, L. Frölich, Olfactory function in mild cognitive impairment and Alzheimer's disease: an investigation using psychophysical and electrophysiological techniques, Am. J. Psychiatr. (2003).

[2] D.P. Perl, Neuropathology of Alzheimer's disease, Mt. Sinai J. Med. 77 (1) (2010 Jan-Feb) 32–42.

[3] S.J. Teipel, E. Cavedo, M.J. Grothe, S. Lista, S. Galluzzi, O. Colliot, M. Chupin, H. Bakardjian, D. Dormont, B. Dubois, H. Hampel, Hippocampus Study Group. Predictors of cognitive decline and treatment response in a clinical trial on suspected prodromal Alzheimer's disease, Neuropharmacology 108 (2016 Sep) 128–135.

[4] R. Petersen, O. Lopez, M. Armstrong, T. Getchius, M. Ganguli, D. Gloss, et al., Practice guideline update summary: mild cognitive impairment, Neurology 90 (3) (2018) 126–135.

[5] R.C. Petersen, R.O. Roberts, D.S. Knopman, B.F. Boeve, Y.E. Geda, R.J. Ivnik, et al., Mild cognitive impairment: ten years later, Arch. Neurol. 66 (December 12) (2009) 1447–5145.

[6] R.C. Petersen, Mild cognitive impairment as a diagnostic entity, J. Intern. Med. 256 (2004) 183–194.

[7] S.G. Mueller, M.W. Weiner, L.J. Thal, R.C. Petersen, C.R. Jack, W. Jagust, J.Q. Trojanowski, A.W. Toga, L. Becket, Ways toward an early diagnosis in Alzheimer's disease: the Alzheimer's disease neuroimaging initiative (ADNI), Alzheimer's Dement. 1 (2005) 55–66.

[8] F. Jessen, S. Wolfsgruber, B. Wiese, H. Bickel, E. Mösch, H. Kaduszkiewicz, M. Pentzek, S.G. Riedel-Heller, T. Luck, A. Fuchs, S. Weyerer, J. Werle, H. van den Bussche, M. Scherer, W. Maier, M. Wagner, German study on aging, cognition and dementia in primary care patients. AD dementia risk in late MCI, in early MCI, and in subjective memory impairment, Alzheimer's Dement. 10 (1) (2014 Jan) 76–83.

[9] Z. Yao, Y. Zhang, L. Lin, et al., Abnormal cortical networks in mild cognitive impairment and Alzheimer's disease, PLoS Comput. Biol. 6 (11) (2010) e1001006, Published 2010 Nov 18.

[10] Jeffrey W. Prescott, Arnaud Guidon, P. Murali Doraiswamy, Kingshuk Roy Choudhury, Chunlei Liu, Jeffrey R. Petrella, Alzheimer's Disease Neuroimaging Initiative, The alzheimer structural connectome: changes in cortical network topology with increased amyloid plaque burden, Radiology 273 (1) (2014) 175–184.

[11] E. Bullmore, O. Sporns, Complex brain networks: graph theoretical analysis of structural and functional systems, Nat. Rev. Neurosci. 10 (3) (2009) 186–198.

[12] C.Y. Lo, P.N. Wang, K.H. Chou, J. Wang, Y. He, C.P. Lin, Diffusion tensor tractography reveals abnormal topological organization in structural cortical networks in Alzheimer's disease, J. Neurosci. 30 (2010) 16876–16885, https://doi.org/10.1523/JNEUROSCI.4136-10.2010.

[13] Y.D. Reijmer, A. Leemans, K. Caeyenberghs, S.M. Heringa, H.L. Koek, G.J. Biessels, et al., Disruption of cerebral networks and cognitive impairment in Alzheimer disease, Neurology 80 (2013) 1370–1377, https://doi.org/10.1212/WNL.0b013e31828c2ee5.

[14] E.T. Bullmore, D.S. Bassett, Brain graphs: graphical models of the human brain connectome, Annu. Rev. Clin. Psychol. 7 (2011) 113–140.

[15] G. Prasad, S.H. Joshi, T.M. Nir, A.W. Toga, P.M. Thompson, Brainconnectivity and novel network measures for Alzheimer's disease classification, Neurobiol. Aging 36 (2015) S121–S131, https://doi.org/10.1016/j.neurobiolaging.2014.04.037.

[16] A. Khvostikov, K. Aderghal, A. Krylov, G. Catheline, J. BenoisPineau, 3D inception-based CNN with sMRI and MD-DTI data fusion for Alzheimer's disease diagnostics, arXiv:1809.03972, 2018.

[17] SinnoJialin Pan, Qiang Yang, A survey on transfer learning, IEEE Trans. Knowl. Data Eng. 22 (10) (2009) 1345–1359.

[18] L. Kang, J. Jiang, J. Huang, T. Zhang, Identifying early mild cognitive impairment by multi modality MRI-based deep learning, Front. Aging Neurosci. (2020).

[19] Eman N. Marzban, et al., Alzheimer's disease diagnosis from diffusion tensor images using convolutional neural networks, PLoS ONE 15 (3) (2020) e0230409.

[20] Eufemia Lella, et al., An ensemble learning approach based on diffusion tensor imaging measures for Alzheimer's disease classification, Electronics 10 (3) (2021) 249.

[21] J. Sheng, B. Wang, Q. Zhang, R. Zhou, L. Wang, Y. Xin, Identifying and characterizing different stages toward Alzheimer's disease using ordered core features and machine learning, Heliyon 7 (6) (2021 Jun 11) e07287.

[22] F. Scarselli, M. Gori, A.C. Tsoi, M. Hagenbuchner, G. Monfardini, The graph neural network model, IEEE Trans. Neural Netw. 20 (2009) 61–80.

[23] T.N. Kipf, M. Welling, Semi-supervised classification with graph convolutional networks, CoRR, arXiv:1609.02907 [abs], 2016.

[24] L. Shao, C. Fu, Y. You, et al., Classification of ASD based on fMRI data with deep learning, Cogn. Neurodyn. (2021).

[25] T. Song, S.R. Chowdhury, F. Yang, H. Jacobs, G.E. Fakhri, Q. Li, K. Johnson, J. Dutta, Graph convolutional neural networks for alzheimers disease classification, in: Proc. IEEE 16th International Symposium on Biomedical Imaging (ISBI), Venezia, Italy, Apr. 2019, pp. 414–417, 21.

[26] Jeremy Kawahara, et al., BrainNetCNN: convolutional neural networks for brain networks; towards predicting neurodevelopment, NeuroImage 146 (2017) 1038–1049.

[27] T. He, et al., Deep neural networks and kernel regression achieve comparable accuracies for functional connectivity prediction of behavior and demographics, NeuroImage 206 (2020) 116276.

[28] H.W. Yeung, S. Luz, S.R. Cox, C.R. Buchanan, H.C. Whalley, K.M. Smith, Pipeline comparisons of convolutional neural networks for structural connectomes: predicting sex across 3,152 participants, Annu. Int. Conf. IEEE Eng. Med. Biol. Soc. 2020 (2020 Jul) 1692–1695.

[29] Paul S. Aisen, et al., Clinical core of the Alzheimer's disease neuroimaging initiative: progress and plans, Alzheimer's Dement. 6 (3) (2010) 239–246.

[30] A. Daducci, S. Gerhard, A. Griffa, A. Lemkaddem, L. Cammoun, X. Gigandet, et al., The connectome mapper: an open-source processing pipeline to map connectomes with MRI, PLoS ONE 7 (12) (2012) e48121.

[31] M. Jenkinson, C.F. Beckmann, T.E. Behrens, M.W. Woolrich, S.M. Smith, FSL, NeuroImage 62 (2012) 782–790.

[32] J.-D. Tournier, F. Calamante, A. Connelly, Improved probabilistic streamlines tractography by 2nd order integration over fibre orientation distributions, ISMRM 88 (2010) 1670.

[33] J.L. Andersson, S.N. Sotiropoulos, An integrated approach to correction for off-resonance effects and subject movement in diffusion MR imaging, NeuroImage 125 (2016) 1063–1078.

[34] R.E. Smith, J.D. Tournier, F. Calamante, A. Connelly, Anatomically-constrained tractography: improved diffusion MRI streamlines tractography through effective use of anatomical information, NeuroImage 62 (3) (2012 Sep) 1924–1938.

[35] R.E. Smith, J-D. Tournier, F. Calamante, A. Connelly, Theeffects of SIFT on the reproducibility and biological accuracy of the structural connectome, NeuroImage 104 (2015) 253–265.

[36] Diederik P. Kingma, Jimmy Ba, Adam: a method for stochastic optimization, preprint, arXiv:1412.6980, 2014.

[37] Nitish Srivastava, et al., Dropout: a simple way to prevent neural networks from overfitting, J. Mach. Learn. Res. 15 (1) (2014) 1929–1958.

[38] E.J. Timothy Behrens, et al., Probabilistic diffusion tractography with multiple fibre orientations: what can we gain?, NeuroImage 34 (1) (2007) 144–155.

[39] Leonardo Bonilha, et al., Reproducibility of the structural brain connectome derived from diffusion tensor imaging, PLoS ONE 10 (9) (2015) e0135247.

[40] Danni Cheng, Manhua Liu, CNNs based multi-modality classification for AD diagnosis, in: 2017 10th International Congress on Image and Signal Processing, Biomedical Engineering and Informatics (CISP-BMEI), IEEE, 2017.

[41] Alzheimer's Disease Neuroimaging Initiative (ADNI), http://adni.loni.usc.edu.

[42] B. Bigham, S.A. Zamanpour, F. Zemorshidi, F. Boroumand, H. Zare, Alzheimer's disease neuroimaging initiative. identification of superficial white matter abnormalities in Alzheimer's disease and mild cognitive impairment using diffusion tensor imaging, J. Alzheimer's Dis. Rep. 4 (1) (2020 Feb 28) 49–59, https://doi.org/10.3233/ADR-190149, PMID:32206757; PMCID:PMC7081087.

[43] Bahare Bigham, et al., Features of the superficial white matter as biomarkers for the detection of Alzheimer's disease and mild cognitive impairment: a diffusion tensor imaging study, Heliyon (2022) e08725.